The FASEB Journal article fj.10-169508. Published online April 25, 2011.

The FASEB Journal • Research Communication

Cell cholesterol modulates metalloproteinase-dependent shedding of low-density lipoprotein receptor-related protein-1 (LRP-1) and clearance function

Charlotte Selvais,* Ludovic D'Auria,* Donatienne Tyteca,* Gwenn Perrot,† Pascale Lemoine,* Linda Troeberg,‡ Stéphane Dedieu,† Agnès Noël,§ Hideaki Nagase,‡ Patrick Henriet,* Pierre J. Courtoy,* Etienne Marbaix,*,[1] and Hervé Emonard†

*Cell Biology Laboratory, de Duve Institute and Université Catholique de Louvain, Bruxelles, Belgium; †Centre National de la Recherche Scientifique (CNRS) Unité Mixte de Recherche (UMR) 6237 and Faculté de Médecine, Université de Reims Champagne-Ardenne, Reims, France; ‡Kennedy Institute of Rheumatology Division, Imperial College London, London, UK; and §Laboratory of Tumor and Developmental Biology, Groupe Interdisciplinaire de Génoprotéomique Appliquée-Cancer, Université de Liège, Liège, Belgium

ABSTRACT **Low-density lipoprotein receptor-related protein-1 (LRP-1) is a plasma membrane scavenger and signaling receptor, composed of a large ligand-binding subunit (515-kDa α-chain) linked to a shorter transmembrane subunit (85-kDa β-chain). LRP-1 cell-surface level and function are controlled by proteolytic shedding of its ectodomain. Here, we identified ectodomain sheddases in human HT1080 cells and demonstrated regulation of the cleavage by cholesterol by comparing the classical fibroblastoid type with a spontaneous epithelioid variant, enriched ~2-fold in cholesterol. Two membrane-associated metalloproteinases were involved in LRP-1 shedding: a disintegrin and metalloproteinase-12 (ADAM-12) and membrane-type 1 matrix metalloproteinase (MT1-MMP). Although both variants expressed similar levels of LRP-1, ADAM-12, MT1-MMP, and specific tissue inhibitor of metalloproteinases-2 (TIMP-2), LRP-1 shedding from epithelioid cells was ~4-fold lower than from fibroblastoid cells. Release of the ectodomain was triggered by cholesterol depletion in epithelioid cells and impaired by cholesterol overload in fibroblastoid cells. Modulation of LRP-1 shedding on clearance was reflected by accumulation of gelatinases (MMP-2 and MMP-9) in the medium. We conclude that cholesterol exerts an important control on LRP-1 levels and function at the plasma membrane by modulating shedding of its ectodomain, and therefore represents a novel regulator of extracellular proteolytic activities.—Selvais, C., D'Auria, L., Tyteca, D., Perrot, G, Lemoine, P., Troeberg, L., Dedieu, S., Noël, A., Nagase, H., Henriet, P., Courtoy, P. J., Marbaix, E., Emonard, H. Cell cholesterol modulates metalloproteinase-dependent shedding of low-density lipoprotein receptor-related protein-1 (LRP-1) and clearance function. *FASEB J.* 25, 000–000 (2011). www.fasebj.org**

Key Words: ADAM · MMP · endocytosis · plasma membrane · raft

LOW-DENSITY LIPOPROTEIN (LDL) receptor-related protein-1 (LRP-1) is a widely expressed membrane receptor, composed of a very large extracellular multiligand-binding subunit (515-kDa α-chain) noncovalently linked to a short-transmembrane subunit (85-kDa β-chain). Both originate from a single 600-kDa type I transmembrane precursor generated by cleavage in the trans-Golgi network by a furin-like convertase. The extracellular domain contains 4 binding modules that mediate endocytic scavenging of a wide variety of proteins, including extracellular matrix regulatory macromolecules, proteinases, and proteinase:inhibitor complexes (for a review, see ref. 1). LRP-1-mediated endocytosis is now recognized as a central mechanism controlling various soluble matrix metalloproteinase (MMP) family members (2). For example, LRP-1-mediated internalization of MMP-2 is pivotal for controlling the extracellular activity of this major proteinase in experimental systems, and we recently extended this conclusion to MMP-2 and MMP-9 in tissue explants from the cycling human endometrium (3), where clearance was regulated by physiological levels of ovarian steroids. We also documented that LRP-1 mediates the endocytic clearance of proMMP-2:tissue inhibitor of metalloproteinases-2 (TIMP-2) complexes in HT1080 fibrosarcoma cells (4).

New roles for LRP-1 in mitogenic and motogenic signal transduction are also emerging, and its crucial function is underlined by embryonic lethality of knockout (KO) mice at embryonic day (E)9 (5). As to LRP-1 mitogenic effects, LRP-1 is tyrosine-phosphorylated by Src, and phosphorylated LRP-1 binds to Shc, an impor-

[1] Correspondence: Cell Biology Laboratory, de Duve Institute, UCL-75.41, 75 avenue Hippocrate, B-1200 Bruxelles, Belgium. E-mail: etienne.marbaix@uclouvain.be

doi: 10.1096/fj.10-169508

This article includes supplemental data. Please visit *http://www.fasebj.org* to obtain this information.

tant adaptor in the activation of Ras signaling pathways (6). *In vitro* and *in vivo* studies also identified LRP-1 as a physiological modulator of platelet-derived growth factor (PDGF) signaling (7). As to LRP-1 motogenic effects, binding of plasminogen activator (PA) inhibitor-1 (PAI-1) to LRP-1 stimulates smooth muscle cell migration *via* JAK/Stat pathway activation (8). LRP-1 can also influence cell motility by controlling the activity of the urokinase-type PA (uPA):uPA receptor system and associated signaling pathways (9). We recently demonstrated that LRP-1 silencing may arrest invasion of carcinoma cells by promoting their substrate attachment (10). Together, either as coreceptor or interacting partner for a number of adaptor proteins, LRP-1 is involved in multiple signaling pathways that regulate migration, invasion, proliferation, vascular permeability, and cell survival (1). Thus, LRP-1 not only is a major endocytic scavenger, thereby downregulating several extracellular events, but also participates in essential intracellular signaling functions.

LRP-1 is controlled at both transcriptional and posttranscriptional levels. LRP-1 expression is regulated by hormones and growth factors, with differential outcomes depending on the cellular context. For example, insulin increases LRP-1 exposure at the hepatocyte cell surface *via* activation of PI3K/Akt signaling (11), but downregulates LRP-1 in macrophages *via* ubiquitination and proteasome degradation (12). However, the main regulation of LRP-1 is achieved by proteolytic shedding or more extensive degradation at the cell surface. Whereas membrane-type MMPs (MT-MMPs) can degrade LRP-1 into low-molecular-mass fragments (13), intact soluble LRP-1 α-chain (sLRP-1) is shed into human plasma (14) and has been identified at the blood-brain barrier on ischemia (15). Characterization of sLRP-1 disclosed copurification with a truncated β-chain of 55 kDa, the predicted molecular mass of the extracellular portion of the β-chain, indicating that LRP-1 shedding occurs by a single cleavage of a membrane-proximal region of this chain (16). Following this observation, various proteolytic enzymes belonging to different proteinase families have been proposed as candidates for LRP-1 shedding, including β-site of amyloid precursor protein (APP)-cleaving enzyme (BACE; ref. 17), tissue-type PA (tPA; ref. 15), a disintegrin and metalloproteinase-10 (ADAM-10; ref. 18) and ADAM-17/tumor necrosis factor-α-converting enzyme (TACE; ref. 18).

In the cycling human endometrium, we noticed temporal restriction of LRP-1 shedding from stromal cells to the menstrual phase, which pointed to a key role of ADAM-12 in this process (3). In the present study, we focused our investigations on human fibrosarcoma HT1080 cells as a model cell system. Indeed, these cells express both LRP-1 (4) and ADAM-12 (19). Moreover, since plasma membrane cholesterol regulates shedding of several transmembrane proteins (20–22), we took advantage of two HT1080 cell variants, with either spontaneous low cholesterol levels (conventional fibroblastoid cells) or high cholesterol levels (epithelioid-type; 2-fold higher cholesterol content). We confirmed that ADAM-12 is necessary for LRP-1 shedding in HT1080 cells and observed that cholesterol prevents LRP-1 shedding, thus favoring clearance of the key gelatinases, MMP-2 and MMP-9.

MATERIALS AND METHODS

Reagents and antibodies

Cell culture medium, fetal calf serum (FCS), and other cell culture reagents were from Life Technologies (Invitrogen, Merelbeke, Belgium). Antibodies raised against the following epitopes were from the indicated suppliers: human LRP-1 515-kDa α-chain (mouse IgG1, clone 8G1) and 85-kDa β-chain (mouse IgG2, clone 5A6), Calbiochem (Merck Chemical Ltd, Nottingham, UK); human transferrin receptor (TfR, mouse IgG1, clone H68.4), Invitrogen; human caveolin-1 (mouse IgG2a, clone 2234/caveolin 1), BD Biosciences (Erembodegem, Belgium); human ADAM-12 (rabbit polyclonal, affinity-purified), Sigma-Aldrich (Bornem, Belgium); human MT1-MMP (rabbit polyclonal, affinity-purified), Chemicon (Millipore, Brussels, Belgium) and glyceraldehyde phosphate dehydrogenase (GAPDH; mouse IgG1, clone 6C5) from Ambion (Austin, TX, USA). Neutralizing goat polyclonal antibodies to ADAM-12 were obtained from Santa Cruz Biotechnology (Heidelberg, Germany), and neutralizing monoclonal antibody to MT1-MMP (mouse IgG2aκ, clone LEM-2/63.1) was obtained from Chemicon. Control nonimmune goat and mouse IgGs were from Dako (Heverlee, Belgium). Nitrocellulose membranes were from Amersham (Roosendaal, The Netherlands). Kaleidoscope SDS-PAGE molecular mass standards were from Bio-Rad (Nazareth, Belgium) and Himark prestained HMW protein standards from Invitrogen. Trypsin was from Worthington (Gestimed, Brussels, Belgium). Complete protease inhibitor cocktail tablets were from Roche (Anderlecht, Belgium). Aminoethylbenzenesulfonyl-fluoride (AEBSF), E64, pepstatin, methyl-β-cyclodextrin (MβCD), lovastatin, cholesterol-loaded MβCD (chol-MβCD), and the 3-[(3-cholamidopropyl) dimethyl-ammonio]-1-propane-sulfonate (CHAPS) detergent were obtained from Sigma-Aldrich. GM6001 and TACE inhibitor (TAPI-1) were from Calbiochem. BB-94 and KB-R7785 were kindly provided by Prof. Y. Okada (Keio University School of Medicine, Tokyo, Japan). Recombinant mouse prodomain of ADAM-10 (rPA10), a specific inhibitor of human ADAM-10 (23), was a generous gift from Dr. M. L. Moss (BioZyme, Apex, NC, USA). Human recombinant TIMP-1 and TIMP-2 were expressed in mammalian cells and purified as described previously (24). The N-terminal domain of human TIMP-3 with a C-terminal His tag was expressed in *Escherichia coli*, folded *in vitro*, and purified (25).

Cell culture

Human fibrosarcoma HT1080 cells, which classically display a fibroblastoid phenotype, were originally purchased from the American Type Culture Collection (Manassas, VA, USA) and grown in DMEM supplemented with 10% (v/v) FCS at 37°C in a humid atmosphere (5% CO_2 and 95% air). After multiple passages, an epithelioid phenotype spontaneously appeared (see Fig. 4*A*) and was selected for comparison with the usual fibroblastoid phenotype of HT1080 cells. For analysis of LRP-1 shedding, cells were grown up to subconfluency in 60-mm Petri dishes, then cultured in the presence or absence of inhibitors or neutralizing antibodies for 24 h in serum-free medium. Cells and conditioned media were collected separately and stored at −20°C prior to analysis.

Confocal microscopy was performed as described previously (26), using 10 μg/ml mouse monoclonal IgG_1 specific for vimentin (Dako) and secondary goat anti-mouse IgG_1 Alexa 488-antibodies (Molecular Probes, Invitrogen).

Transfection of small interfering RNA (siRNA)

The 21-base oligonucleotides targeting ADAM-12, AACGGGAAAGCAAAGAACUTT (27) and GGAAGAGCUGAUGAAGUUGTT (28) and their complementary sequences were synthesized by Eurogentec (Seraing, Belgium). The two siRNAs targeting MT1-MMP (29) were kindly provided by Dr. F. Antonicelli (Faculté de Médecine, Reims, France). siRNA negative control duplexes were from Eurogentec. Transfection was performed using Lipofectamine 2000 (Invitrogen), according to the manufacturer's instructions. HT1080 cells were transfected twice at 15-h intervals to increase silencing efficiency, and assays were performed 24 h after the second transfection. To test for specificity, MT1-MMP expression was evaluated by Western blotting in ADAM-12-knockdown cells and *vice versa*. Cellular LRP-1 protein levels were monitored in parallel.

Real-time PCR

Aliquots of 200 ng total RNA were extracted using the SV Total RNA Isolation System (Promega, Leiden, The Netherlands) and reverse-transcribed by using the oligo(dT) protocol of the Thermoscript RT-PCR system (Invitrogen). For PCR, the oligonucleotide primers and TaqMan probes were designed as reported previously: ADAM-10 and TACE (30); LRP-1 (31); membrane-anchored splice variant mRNA of ADAM-12 (ADAM-12m; ref. 32); MT1-MMP (33); TIMPs (34), and β-actin (35). Customized primers were obtained from Invitrogen. Standards for quantitative PCR amplification were as reported previously (34). Real-time PCR was performed as described previously (3).

Cell-surface trypsinization

Confluent fibroblastoid and epithelioid HT1080 cells were washed twice with ice-cold PBS, then surface-digested with 0.5% (w/v) trypsin in PBS at 4°C for 45 min on a rocking platform. After 3 washes with PBS, digestion was stopped by adding FCS (200 μl in 2-ml suspended cells, 10 min at 4°C). Control cells were scraped in 2 ml of cold PBS. After careful rinsing (4 times with cold PBS, on ice), trypsinized and control cells were lysed in 0.01% (v/v) Triton X-100 and sonicated on ice (3×10 s) for Western blot analysis of LRP-1 α-chain.

Cell-surface biotinylation

Fibroblastoid and epithelioid HT1080 cells were washed twice with cold PBS, then incubated with sulfo-NHS-LC-biotin (0.5 mg/ml; Thermo Scientific; Fisher Scientific, Illkirch, France) for 30 min. After rinsing twice with cold PBS, cells were incubated with 100 mM glycine for 30 min. After further washing (3 times with cold PBS), cells were scraped in lysis buffer (10 mM Tris-HCl buffer, pH 7.2, containing 150 mM NaCl, 1% v/v Triton X-100, 5 mM EDTA, 0.1 mM sodium orthovanadate, and Complete protease inhibitor cocktail) and incubated on ice for additional 30 min, under agitation. Cell extracts were pelleted at 10,000 *g* at 4°C for 10 min. After quantification using the microbicinchoninic acid assay (Pierce; Fisher Scientific), solubilized proteins (1 mg) were incubated with streptavidin-coated agarose beads (Thermo Scientific) at 4°C overnight. After washing 3 times with lysis buffer to remove nonspecific binding, beads were boiled in SDS-electrophoresis sample buffer for 5 min, then centrifuged at 10,000 *g* at 4°C for 10 min. Supernatants were analyzed by Western blot analysis.

Cellular cholesterol modulation and assay

Epithelioid HT1080 cells were cholesterol depleted either by direct extraction with MβCD (36) or on HMG-CoA reductase inhibition by lovastatin (22). Subconfluent cells plated onto 60-mm Petri dishes were treated with 5 mM MβCD in FCS-free medium for 30 min, washed with PBS, then further incubated in FCS-free medium for 1 or 6 h. Alternatively, dishes were treated with 15 μg/ml lovastatin in FCS-free medium for 24 h. In both cases, control cells were treated with vehicle alone. Conversely, fibroblastoid HT1080 cells were overloaded with cholesterol on incubation with 1 mM chol-MβCD in DMEM with 10% FCS for 90 min. Cells were washed with PBS, then further incubated in FCS-free medium for 1 or 6 h. Six-hour conditioned media (for MβCD and chol-MβCD treatments), and 24-h conditioned media (for lovastatin treatment) were concentrated, and shedding of LRP-1 was analyzed by Western blotting. Cellular cholesterol was extracted and purified by a procedure derived from the protocol of Bligh and Dyer (37). Briefly, cells were harvested in water, and the lipids were extracted with 3 vol of chloroform/methanol (2:1; v/v), stirred 1 min, and centrifuged at 1760 *g* for 15 min. The organic phase was collected and washed with 2 vol of 0.05 M NaCl, then twice with 2 vol of 0.36 M $CaCl_2$/methanol solution (1:1; v/v), and stirred and centrifuged at each wash. The organic phase was again collected and dried under argon, then solubilized in 0.5% Triton X-100. Free cholesterol was estimated using the cholesterol oxidase-base Amplex Red Cholesterol Assay kit (Molecular Probes; Invitrogen) with omission of the prior cholesterol esterase step. Effects of cholesterol modulation on MMP-2 and MMP-9 activity were analyzed by gelatin zymography of concentrated medium conditioned for 1 h.

Triton X-100 solubility-based protein fractionation

Confluent fibroblastoid and epithelioid HT1080 cells were harvested from 150-mm Petri dishes and extracted in 1% Triton X-100 containing protease inhibitors for 30 min at 4°C (38). The extracts were centrifuged at 12,000 *g* for 20 min at 4°C. Supernatants were collected as the Triton X-100-soluble fractions. The Triton X-100-insoluble pellets were suspended in ice-cold lysate buffer (PBS containing 1% Triton X-100, 0.5% sodium deoxycholate, 0.1% SDS and complete protease inhibitor cocktail) and sonicated on ice (3×10 s). Both Triton X-100-insoluble and -soluble fractions were analyzed by Western blot.

Western blot and zymographic analyses

Western blotting was performed as described previously(3) using 5% polyacrylamide minigels for LRP-1 515-kDa α-chain and 10% polyacrylamide minigels for the other proteins. Primary antibodies were used at a concentration of 1 μg/ml for LRP-1 α- and β-chains, MT1-MMP and TfR, 0.5 μg/ml for ADAM-12 and GAPDH, and 0.25 μg/ml for caveolin-1. Conditioned media were concentrated 10-fold with Amicon Centrifugal Filter Devices (Millipore) following the manufacturer's recommendations. Samples were normalized with respect to DNA concentration, which was measured by intercalation of 0.5 μg/ml diamino-2-phenylindole (Sigma-Aldrich) and spectrophotometry at 460 nm. Each lane was loaded with cell lysates equivalent to 5 μg DNA, or corresponding amounts of conditioned medium. Immunoreactive bands were visualized using chemiluminescence (ECL advance Western blotting

detection kit, Amersham), acquired using a 2000MM Kodak Image Station (Eastman Kodak Company, Rochester, NY, USA), and quantified using Kodak 1D Image Analysis software. Gelatin zymography (8% polyacrylamide gel) was performed as described previously (3).

Statistical analysis

Statistical analysis was performed using either a 2-factor analysis of the variance (2-way ANOVA) and *post hoc* Student's *t* test or only a Student's *t* test when ANOVA was not relevant. Differences were considered significant for $P < 0.05$. Values are reported as means ± SD.

RESULTS

The LRP-1 ectodomain is abundantly shed by HT1080 human fibrosarcoma cells

We selected the HT1080 human fibrosarcoma cell line as a well-established *in vitro* model of cells expressing LRP-1 at high levels (4), exceeding that of β-actin mRNA (see below, Fig. 4*B*). In media conditioned for 24 h of cell culture, the α-chain was detected by immunoblotting as a major 515-kDa band corresponding to the intact protein found in cell lysates. It was accompanied by bands corresponding to a single degradation product of ~300 kDa (**Figs. 1*A*, *B***) and a 55-kDa truncated fragment of the β-chain (Fig. 1*B*). These data suggested that the level of plasma membrane-associated LRP-1 in these cells was largely regulated by shedding of the ectodomain resulting from cleavage of the β-chain in close vicinity of the plasma membrane (Fig. 1*C*), as recently described in human endometrial stromal cells (3). GM6001, a broad-spectrum metalloproteinase inhibitor, strongly reduced the levels of both the intact α-chain and the extracellular part of β-chain released in conditioned medium (Fig. 1*B*), accompanied with a corresponding increase of LRP-1 α-chain in cell lysates (Fig. 1*A*). To explore whether shedding essentially occurred at the cell surface or after endocytosis of LRP-1 linked to a metalloproteinase, followed by intracellular hydrolysis and release of the LRP-1 ectodomain, we aimed at blocking endocytosis by ATP depletion (26). As shown in Supplemental Fig. S1*A–D*, the treatment abolished receptor-mediated transferrin endocytosis, while shedding of LRP-1 α-chain was not inhibited and even slightly increased (Supplemental Fig. S1*E*). These data indicated that shedding of the ectodomain essentially resulted from proteolysis at the cell surface.

LRP-1 ectodomain is shed by a metalloproteinase

To identify the proteolytic enzymes responsible of the LRP-1 shedding, we first screened inhibitors against the different classes of proteolytic enzymes. The release of the LRP-1 ectodomain was severely impaired by two broad-spectrum metalloproteinase inhibitors, GM6001 and BB-94, but not by cysteine (E64), serine (AEBSF), or aspartyl proteinase (pepstatin) inhibitors (**Fig. 2*A***). Shedding was also partially decreased by the ADAM-selective inhibitor, KB-R7785 (refs. 28, 39; Fig. 2*A*). These results demonstrated that LRP-1 ectodomain was shed by a metalloproteinase, possibly an ADAM, as previously suggested (3). To explore the possible proteases involved, we first focused on ADAM-10 and ADAM-17 (TACE). Indeed, these two metalloproteinases are known to cleave various ectodomains (40), and both are expressed by HT1080 cells at mRNA levels corresponding to ~1% of β-actin mRNA (data not shown). However, LRP-1 ectodomain shedding was insensitive to rPA10, a specific inhibitor of ADAM-10 (23) and to TAPI-1, a potent inhibitor of TACE (41) (Fig. 2*B*). Therefore, we examined the effect of TIMPs, which can inhibit both MMPs and ADAMs, with different responses indicative of the nature of the protease involved (42). LRP-1 shedding was insensitive to TIMP-1 (90±10% of controls, mean±SD of 3 indepen-

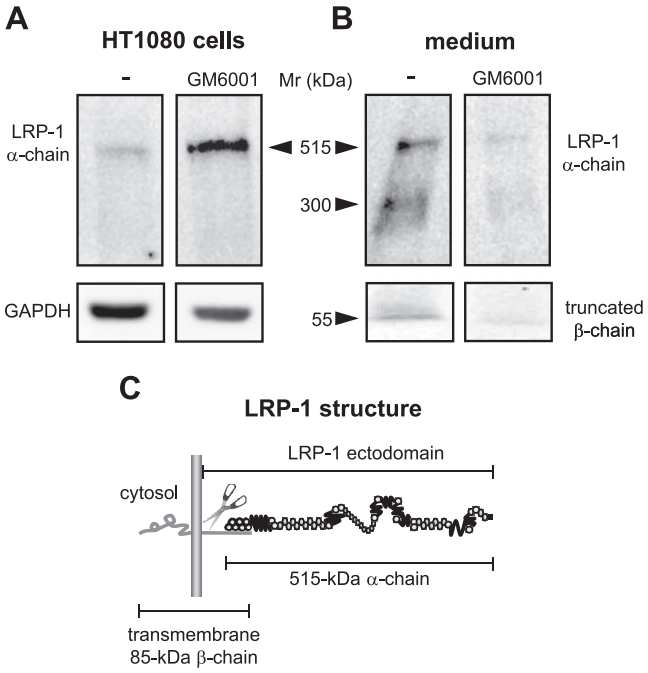

Figure 1. LRP-1 ectodomain is shed by cleavage of the β-chain in human fibrosarcoma HT1080 cells. Cells were cultured for 24 h in serum-free DMEM, in the absence or presence of the metalloproteinase inhibitor GM6001 (10 μM). *A*) Western blotting of LRP-1 α-chain in cell lysates. Full-length α-chain is more abundant in the cells treated by GM6001 (right lane) than in the untreated cells (left lane). Blot is representative of 8. *B*) Western blotting of LRP-1 α- and β-chains in culture medium conditioned for 24 h. LRP-1 α-chain is accompanied by a single 300-kDa degradation product and by a β-chain fragment of 55 kDa, corresponding to the extracellular portion of the β-chain. Concentrated conditioned media were normalized to the DNA content of the corresponding cell layers. Abundance of both chains is largely and proportionally decreased in medium conditioned in the presence of GM6001 (representative of 8 blots). *C*) Domain structure of LRP-1 illustrates how cleavage of the extracellular portion of the β chain, in close vicinity of the plasma membrane, releases the LRP-1 ectodomain (55-kDa truncated β-chain and full-length 515-kDa α-chain).

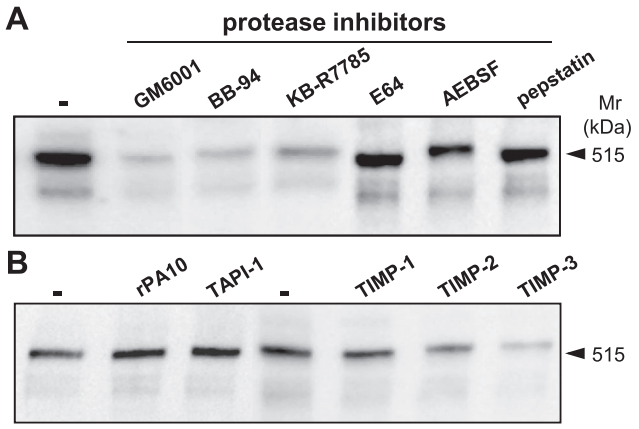

Figure 2. Effect of protease inhibitors on LRP-1 ectodomain shedding. Western blotting of LRP-1 α-chain in media conditioned for 24 h by fibroblastoid HT1080 cells. *A*) Cells were cultured without (−) or with broad-spectrum inhibitors of metalloproteinases (10 μM GM6001; 1 μM BB-94), ADAMs (1 μM KB-R7785), cysteine proteinases (20 μM E64), serine proteinases (100 μM AEBSF), or aspartyl proteinases (15 μM pepstatin). *B*) Cells were cultured without or with a specific inhibitor of ADAM-10 (10 μM rPA), of ADAM-17 (10 μM TAPI-1) or 1 μM human recombinant TIMP-1, TIMP-2, or N-terminal domain of TIMP-3.

dent experiments, NS), partially impaired by TIMP-2 (60±15% of controls, $P<0.05$) and strongly inhibited by TIMP-3 (30±8% of controls, $P<0.0005$) (Fig. 2*B*). ADAM-12 is the only member of the ADAM subfamily to be specifically inhibited by TIMP-2 and TIMP-3 (43), but this property is shared by MT1-MMP (44). To the best of our knowledge, the effect of KB-R7785 on MT1-MMP is unknown, and this second candidate could, therefore, not be excluded.

Both ADAM-12 and MT1-MMP are major sheddases of LRP-1 ectodomain

To clarify the respective contribution of ADAM-12 and MT1-MMP on LRP-1 ectodomain shedding, we tested the effect of blocking antibodies and siRNAs (**Fig. 3**). Western blotting revealed that a blocking anti-ADAM-12 antibody (28) strongly increased (~3 fold) LRP-1 α-chain abundance in cell lysates as compared with an irrelevant antibody (Fig. 3*A*). Blocking anti-MT1-MMP antibody (45) also specifically increased the cell signal, albeit less efficiently than the anti-ADAM-12 antibody (Fig. 3*B*). These data indicated that both candidates qualified as LRP-1 ectodomain sheddases. As a second approach, we performed siRNA-mediated knockdown experiments. Two siRNAs used for each candidate sheddase decreased ADAM-12 (Fig. 3*C*) or MT1-MMP (Fig. 3*D*) protein levels. Knockdown of each putative sheddase induced a strong increase in LRP-1 α-chain levels in cell lysates, and a corresponding decrease in the conditioned medium was seen (Fig. 3*C, D*). As a control of specificity, siRNA for ADAM-12 had no effect on MT1-MMP expression (Fig. 3*C*). Decreased expression of MT1-MMP was accompanied by a lower level of the active form (92 kDa) of ADAM-12 (Fig. 3*D*), consistent with a role of the former in ADAM-12 maturation.

LRP-1 ectodomain shedding is impaired in epithelioid HT1080 cells

Human fibrosarcoma HT1080 cells can spontaneously convert into an epithelioid variant (46). The classical fibroblastoid variant featured elongated cells with frequent overlaps, whereas the epithelioid variant showed

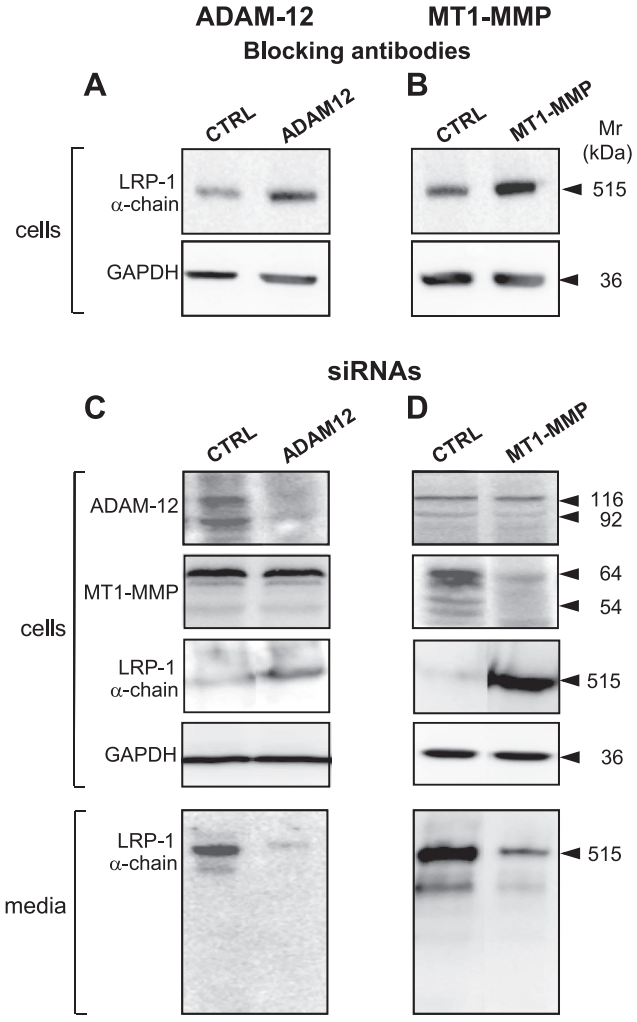

Figure 3. ADAM-12 and MT1-MMP blocking antibodies or siRNA silencing prevent shedding of the LRP-1 ectodomain. *A, B*) Blocking antibodies: Western blotting of LRP-1 α-chain and GAPDH in lysates of fibroblastoid HT1080 cells treated for 24 h with 10 μg/ml anti-ADAM-12 antibodies (*A*) or nonimmune goat IgG control (CTRL); or 5 μg/ml anti-MT1-MMP antibody (*B*) or nonimmune mouse IgG control. *C, D*) Efficiency and specificity of siRNAs targeting ADAM-12 (*C*) or MT1-MMP (*D*). Fibroblastoid HT1080 cells were treated as described under Materials and Methods with 100 nM-specific siRNA or negative controls. Western blotting of ADAM-12, MT1-MMP, LRP-1 α-chain, and GAPDH was performed in cell lysates, and blotting of LRP-1 α-chain in corresponding amounts of 24-h conditioned medium. Data are from a representative experiment for the most effective siRNA against each target. All experiments were performed at least twice in triplicate.

lengthy continuous contacts, without overlap (**Fig. 4*A***). Comparable vimentin immunolabeling confirmed that fibroblastoid-to-epithelioid variation did not affect the mesenchymal phenotype (inserts at Fig. 4*A*). LRP-1 mRNA levels did not vary significantly between fibroblastoid and epithelioid HT1080 cells (Fig. 4*B*). However, epithelioid cells contained 1.7 ± 0.6-fold more LRP-1 α-chain than fibroblastoid cells (n=7 experiments, P<0.05) and released 2.8 ± 0.3-fold less LRP-1 α-chain than fibroblastoid cells in medium (P<0.0005) (Fig. 4*C*). Reduced shedding observed in epithelioid cells could result from higher levels of intracellular LRP-1. To test this hypothesis, we discriminated the cell-surface pool of LRP-1 content by trypsinization and surface biotinylation of epithelioid and fibroblastoid cells. After efficient trypsinization (Supplemental Fig. S2), the LRP-1 level was significantly reduced (P<0.005) in both HT1080 variants (Fig. 4*D*) but residual, *i.e.*, intracellular, LRP-1 was similar (P=0.35) in epithelioid cells (30.3±22.6% of total LRP-1; n=8) and fibroblastoid cells (21.4±6.4%; n=8). Biotinylation experiment revealed that epithelioid cell-surface exhibited 2.1 ± 0.3-fold more LRP-1 α-chain than fibroblastoid cells (n=8, P<0.0005; Fig. 4*E*). These data clearly demonstrate much-reduced shedding efficiency in epithelioid HT1080 cells.

Impaired LRP-1 ectodomain shedding in the epithelioid variant cannot be explained by differential expression of sheddases or TIMPs

To test whether the decreased LRP-1 ectodomain shedding observed in epithelioid cells merely reflected a lower protease or a higher antiprotease activity, we first compared the expression profiles of the two key sheddases, ADAM-12 and MT1-MMP (**Fig. 5**). No significant difference was found in mRNA levels between the two variants (Fig. 5*A*). For both sheddases, protein content and activation state were slightly increased in the epithelioid variant (Fig. 5*B*), ruling out that decrease of shedding was due to decreased sheddase expression. Therefore, we examined whether the activity of the two proteinases was differentially regulated by TIMPs in the two variants. TIMP-1 and TIMP-2 mRNA levels were indistinguishable between the two variants, and TIMP-3 mRNA was not detected (Fig. 5*C*). Thus, increased shedding of LRP-1 in the fibroblastoid cells could not be explained by an increased expression or activation of ADAM-12 and MT1-MMP, or by a decreased inhibition of the proteinases.

Cellular cholesterol level is a major regulator of LRP-1 shedding

Since cholesterol can regulate membrane receptor shedding (20–22), we investigated whether differences in cholesterol content could account for unequal LRP-1 ectodomain shedding between the two HT1080 variants (**Fig. 6**). Remarkably, much higher cholesterol content (~2 fold) was found in epithelioid as compared with fibroblastoid HT1080 cells (Fig. 6*A*). This observation prompted us to investigate the effect of cholesterol manipulation on LRP-1 shedding. This was achieved by acute cholesterol depletion with empty MβCD, by acute cholesterol overload with cholesterol-loaded MβCD, or

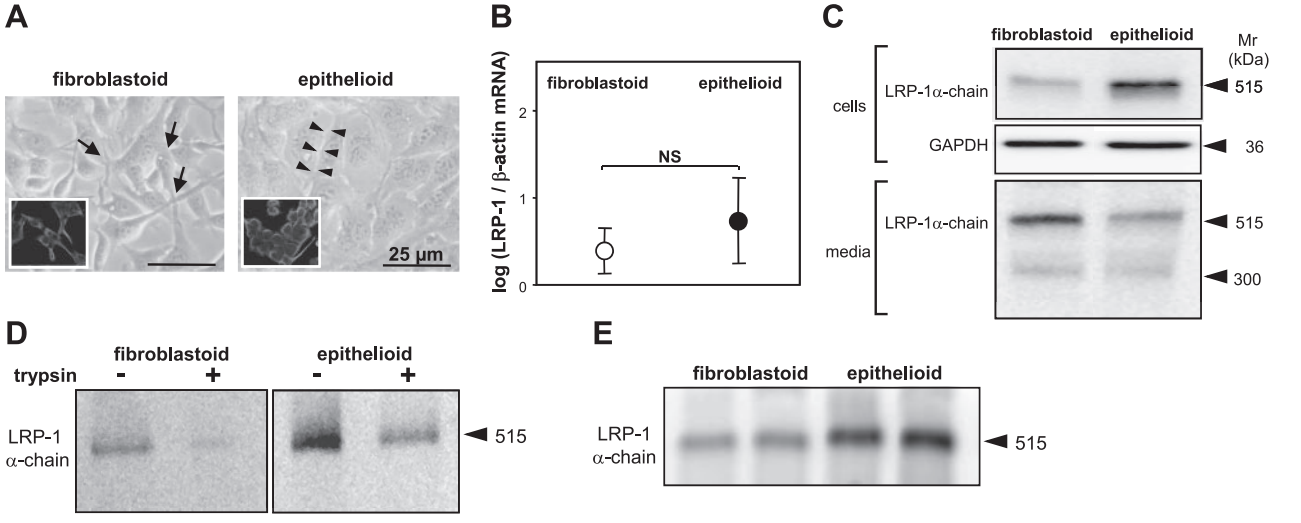

Figure 4. Shedding of LRP-1 ectodomain is decreased in epithelioid HT1080 cell variant. *A*) Microscopic appearance of fibroblastoid and epithelioid phenotypes. Left panel: arrows point to cell overlaps in the fibroblastoid variant. Right panel: paired arrowheads indicate close parallel membrane apposition in the epithelioid variant. Insets: comparable vimentin immunolabeling in the two variants. *B*) Quantitative real-time RT-PCR of LRP-1 mRNAs in fibroblastoid and epithelioid variants, showing comparable levels of expression normalized to β-actin mRNA (mean ± SD log of ratios, n=8). *C*) Western blotting of LRP-1 α-chain and GAPDH in lysates of fibroblastoid and epithelioid variants and of LRP-1 α-chain in the corresponding 24-h conditioned medium. Blots are representative of 7 experiments performed in triplicate. *D*) Western blotting of LRP-1 α-chain in lysates of fibroblastoid and epithelioid variants after trypsinization assay. Blots are representative of 2 experiments performed in quadruplicate. *E*) Streptavidin pulldown of biotinylated cell-surface LRP-1 α-chain from lysates of fibroblastoid and epithelioid variants. Western blots are representative of 2 experiments performed in quadruplicate. NS, not significant, using Student's t test.

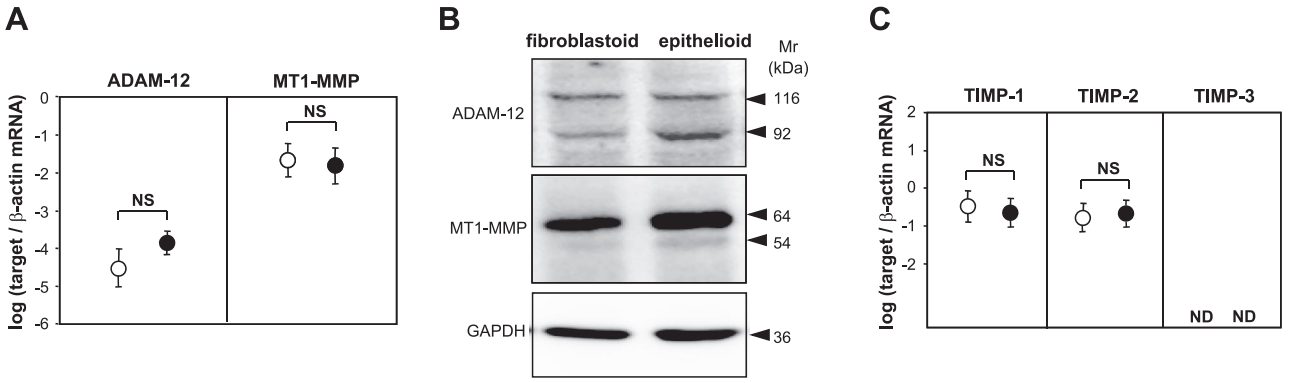

Figure 5. Sheddase and TIMP expression levels are comparable in the two HT1080 cell variants. *A*) Quantitative real-time RT-PCR of ADAM-12 and MT1-MMP mRNA levels, normalized to β-actin mRNA (open circles, fibroblastoid cells; solid circles, epithelioid cells; $n=4$). *B*) Western blotting of ADAM-12, MT1-MMP, and GAPDH in lysates of the two cell variants (representative of 3 blots). *C*) Quantitative real-time RT-PCR of TIMP-1, TIMP-2, and TIMP-3 mRNA levels, normalized to β-actin mRNA ($n=3$). TIMP-3 mRNA was below the level of detection. ND, not detected; NS, not significant, using Student's *t* test. Data are presented as mean ± SD log of ratios.

by 24-h inhibition of cholesterol biosynthesis by the HMG-CoA reductase inhibitor, lovastatin. Whereas MβCD treatment affected neither cholesterol levels (Fig. 6*A*) nor shedding (Fig. 6*B*) in fibroblastoid cells, it strongly depleted epithelioid cell cholesterol content (Fig. 6*A*) and increased LRP-1 shedding to levels ob-

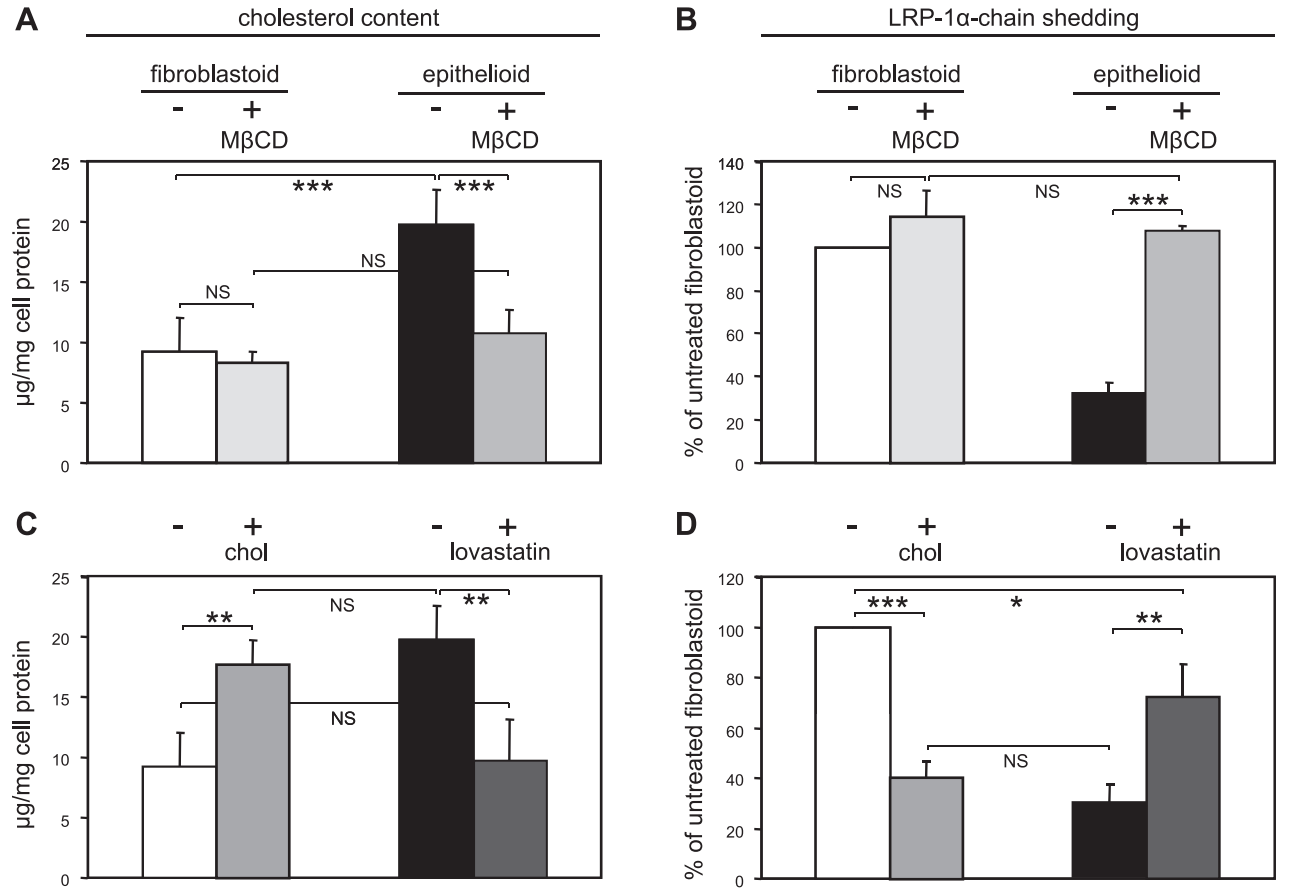

Figure 6. Cellular cholesterol levels regulate metalloproteinase-dependent shedding of LRP-1 ectodomain. Cholesterol content (*A*, *C*) was measured in the two HT1080 variants; LRP-1 ectodomain shedding (*B*, *D*) was quantified on Western blots of α-chain released in the corresponding concentrated medium conditioned for 6 h (or 24 h for lovastatin treatment; data normalized as a percentage of untreated fibroblastoid cells) as described in Materials and Methods. *A*, *B*) Effect of acute cholesterol depletion. Fibroblastoid and epithelioid HT1080 cells were treated without (−) or with (+) 5 mM empty MβCD for 30 min ($n=6$). *C*, *D*) Cholesterol was enriched in fibroblastoid cells by exogenous supply with 1 mM chol-MβCD for 90 min (+ chol; $n=3$). Alternatively, cholesterol was metabolically depleted in epithelioid HT1080 cells by treatment with 4 μM lovastatin for 24 h ($n=5$). NS, not significant. Values are means ± SD. $^*P < 0.05$, $^{**}P < 0.005$, $^{***}P < 0.0005$; Student's *t* test.

served in fibroblastoid cells (Fig. 6*B*). As negative controls, treatment of epithelioid cells with αCD or γCD, which both display no affinity for cholesterol (47), had no effect on cell cholesterol content or on LRP-1 shedding (Supplemental Fig. S3*A, B*). Interestingly βCD, a less potent cholesterol extractor than MβCD (48), increased LRP-1 shedding in epithelioid cells but to a lower extent than MβCD (Supplemental Fig. S3). Likewise, lovastatin treatment of epithelioid cells decreased cholesterol content to levels of fibroblastoid cells (Fig. 6*C*) and promoted LRP-1 shedding (Fig. 6*D*). Conversely, cholesterol enrichment of fibroblastoid cells by MβCD-cholesterol complex (Fig. 6*C*) decreased LRP-1 shedding (Fig. 6*D*). Taken together, these data clearly indicated that cell cholesterol content inversely correlated with LRP-1 ectodomain shedding by ADAM-12 and MT1-MMP.

Differential LRP-1 ectodomain shedding in the cholesterol-poor fibroblastoid and cholesterol-rich epithelioid HT1080 cells cannot be explained by difference in membrane localization of LRP-1 and sheddases

Since cell cholesterol appears to regulate LRP-1 ectodomain shedding, we looked for a differential distribution of LRP-1, MT1-MMP, and ADAM-12 in cholesterol-rich microdomains, such as plasma membrane rafts, in the two HT1080 variants by Triton X-100 solubility-based fractionation of proteins (38). In both HT1080 variants, LRP-1 α-chain was exclusively retrieved in the cold Triton X-100-soluble fractions, like the transferrin receptor, and segregated from MT1-MMP, which partially partitioned in the cold Triton X-100-insoluble pellet, like the raft-localized caveolin-1 (**Fig. 7*A***). Similarly, ADAM-12 was predominantly detergent insoluble. We verified that no LRP-1 could be found in the insoluble pellet when shedding was inhibited by GM6001 in fibroblastoid cells (data not shown) as well as epithelioid cells (Fig. 7). Furthermore, cholesterol unloading of epithelioid HT1080 cells by MβCD did not modify distribution of LRP-1 and its sheddases (Fig. 7*B*). These data indicate that difference of LRP-1 ectodomain shedding between the cholesterol-poor fibroblastoid and the cholesterol-rich epithelioid HT1080 cells cannot be explained by differential compartmentalization of LRP-1 and its dedicated sheddases at the plasma membrane.

Cellular cholesterol regulates LRP-1-mediated clearance

We recently reported that LRP-1 shedding is an important post-translational regulatory mechanism for MMPs activity in the human endometrium (3). We therefore exploited the HT1080 model to test whether modulation of LRP-1 ectodomain shedding by cellular cholesterol would affect the clearance of two major MMPs, MMP-2 and MMP-9 (**Fig. 8**). In medium conditioned by fibroblastoid cells, gelatin zymography revealed a decrease of both MMP-2 and MMP-9 activities on cholesterol enrichment. In contrast, cholesterol depletion increased MMP-2 and MMP-9 activities in medium conditioned by epithelioid cells. Moreover, MβCD treatment induced proMMP-2 activation (Fig. 8*A*), as described previously (49).

DISCUSSION

In this study, we demonstrated that LRP-1 undergoes a major shedding in conventional fibroblastoid HT1080 human fibrosarcoma cells, and we identified two transmembrane metalloproteinases, ADAM-12 and MT1-MMP, as LRP-1 ectodomain sheddases. The serendipitous observation that LRP-1 ectodomain shedding was markedly reduced in an epithelioid variant, despite similar amounts of ADAM-12, MT1-MMP, and TIMP-2,

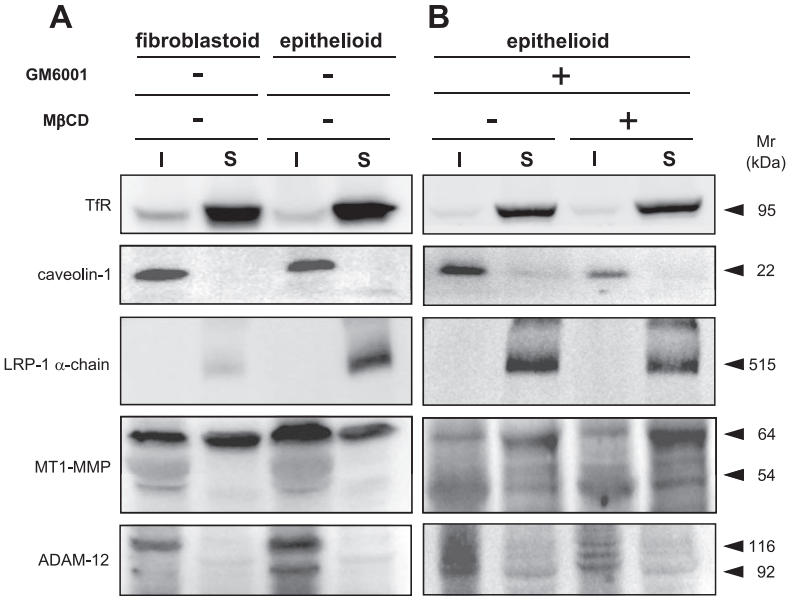

Figure 7. The two HT1080 cell variants show similar distribution of LRP-1, MT1-MMP, and ADAM-12 in Triton X-100 solubility-based fractions. Cells were extracted in cold Triton X-100 as described in Materials and Methods. *A*) Untreated (−) fibroblastoid and epithelioid HT1080 cells. *B*) Epithelioid cells were treated without (−) or with (+) MβCD to deplete cholesterol. Note that 10 μM GM6001 was added throughout the experiment to block LRP-1 ectodomain shedding. Western blotting of LRP-1 α-chain, MT1-MMP, and ADAM-12 in Triton X-100-insoluble (I) and -soluble (S) fractions of fibroblastoid and epithelioid HT1080 cells. TfR and caveolin-1 are markers of Triton X-100-soluble and -insoluble fractions, respectively. Each experimental condition was tested at least twice.

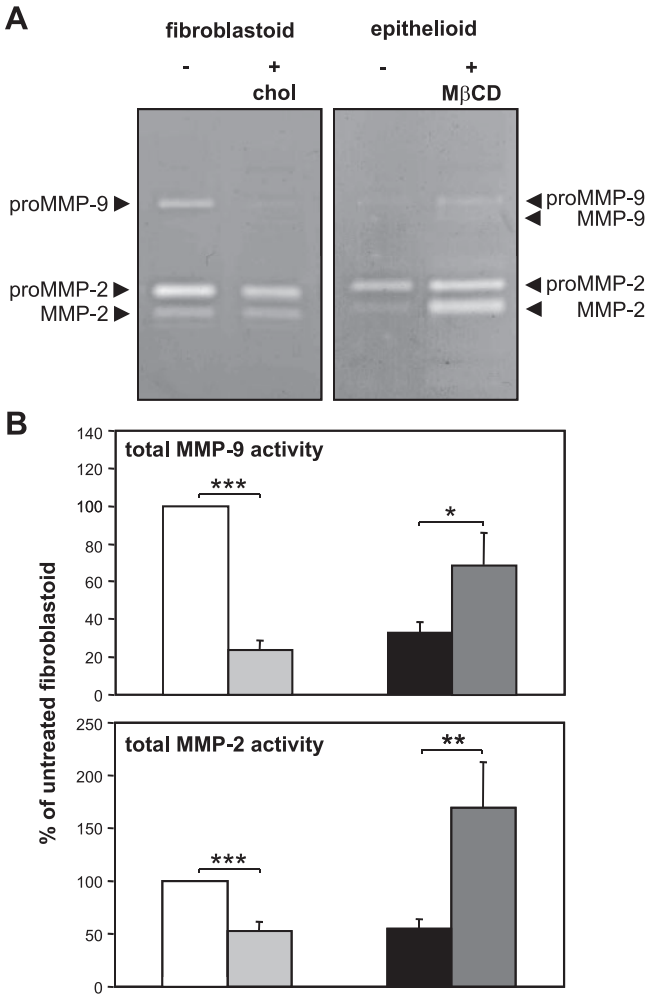

Figure 8. Cellular cholesterol regulates MMP-2 and MMP-9 clearance. Cholesterol was enriched in fibroblastoid cells by treatment with chol-MβCD (+ chol) and was depleted in epithelioid cells by treatment with empty MβCD. Concentrated media conditioned for 1 h were analyzed by gelatin zymography. *A*) Representative zymograms from 4 experiments. *B*) Quantification of total gelatinase activities (latent and active forms) normalized to untreated fibroblastoid cells (n=4). $^*P < 0.05$, $^{**}P < 0.005$, $^{***}P < 0.0005$; Student's t test.

allowed us to unravel membrane cholesterol as the key regulator. Indeed, cholesterol content was ~2-fold higher in epithelioid cells; cholesterol depletion restored their shedding activity to a level comparable to the fibroblastoid cells; and, conversely, cholesterol enrichment of the fibroblastoid cells strongly impaired LRP-1 ectodomain shedding.

Various membrane-bound proteases can cause LRP-1 ectodomain shedding from the cell surface. In the brain, the aspartyl-protease BACE-1 (17) and the serine-protease tPA (15) were originally reported to be responsible for LRP-1 shedding. However, LRP-1 release in the conditioned medium of HT1080 cells was not prevented either by pepstatin or by AEBSF, respective aspartyl- and serine-proteinase inhibitors. In sharp contrast, shedding was largely prevented by the metalloproteinase inhibitors GM6001 and BB-94 and by an ADAM inhibitor, KB-R7785, pointing to a role of an ADAM in the LRP-1 shedding process. ADAM-10 and TACE are known to cause ectodomain shedding (50), including recent evidence for LRP-1 in the brain (18). Although ADAM-10 and TACE are expressed at a higher level than ADAM-12 in HT1080 cells, they are not involved in LRP-1 ectodomain shedding in these cells. Indeed, ADAM-10 is inhibited by TIMP-1 (50), which had no effect on LRP-1 ectodomain shedding by HT1080 cells, while TACE is not sensitive to TIMP-2 (40). Moreover, specific inhibitors of ADAM-10 (23) and TACE (41) did not inhibit shedding. The TIMP inhibitory profile (TIMP-3>TIMP-2>TIMP-1) rather favors a role for ADAM-12 (43), a broad-spectrum sheddase (for a review, see ref. 51), and MT1-MMP (44). HT1080 cells that overexpress MT1-MMP or are stimulated by phorbol esters were reported to degrade LRP-1 α-chain into small fragments (13). In our experimental conditions, such an extensive fragmentation did not occur, indicating that MT1-MMP can efficiently shed LRP-1 without any degradation, as previously reported for the receptor activator of the NF-κB ligand, RANKL (52). Neutralizing antibodies and knockdown experiments confirmed that both ADAM-12 and MT1-MMP are involved in LRP-1 ectodomain shedding. These two sheddases are probably not redundant. Although ADAM-12 bears a furin-recognition site at the end of the propeptide domain and is thus activated intracellularly by proprotein convertases such as furin, the cleaved prodomain remains associated with the mature enzyme (53). This might influence the catalytic capacity of ADAM-12 in the pericellular space and suggests synergy with MT1-MMP. Indeed, by cleaving the ADAM-12 prodomain at the cell surface, MT1-MMP could promote ADAM-12 sheddase activity. This hypothesis is supported by our observation that the decrease of MT1-MMP levels is accompanied by decreased amounts of active ADAM-12 (Fig. 3*D*). Alternatively, the intracellular domain of MT1-MMP (54) could favor interactions between ADAM-12 and intracellular proteins, such as PACSIN3 (55) or Eve-1 (19), thereby improving its sheddase activity.

A major finding was the regulation of shedding by cholesterol, for which the comparison of the two HT1080 variants proved informative. Although fibroblastoid and epithelioid variants showed comparable levels of sheddases and of their inhibitors, LRP-1 ectodomain shedding markedly differed. Such a discrepancy suggests that regulation by topology occurs in the shedding process. Release of numerous ADAM substrates, such as APP (20), interleukin-6 receptor (21) and CD30 (22) is increased following cholesterol depletion by MβCD. Amyloidogenic processing of APP mediated by β- and γ-secretase has been proposed to reflect APP localization in lipid rafts and to depend on endocytosis (56). Interestingly, cholesterol depletion, which inhibited amyloidogenic processing, stimulated a nonamyloidogenic processing by α-secretase, which generates soluble APP ectodomain, presumably outside lipid rafts (20, 56). Likewise, we found that cholesterol

depletion greatly increased the release of the LRP-1 ectodomain from the epithelioid HT1080 cell surface. LRP-1 has been reported to be partially and transiently located into rafts in HT1080 cells (38). Altogether, our results and these reported data are compatible with the hypothesis that an "amyloidogenic"-like process of LRP-1 could occur in lipid rafts of cholesterol-rich epithelioid HT1080 cells, whereas soluble LRP-1 ectodomain generated in fibroblastoid cells with low cholesterol content would result from LRP-1 cleavage outside the lipid rafts. Although the structure of the plasma membrane is totally reorganized after cold Triton X-100 treatment (38), our data lend support to a segregation between LRP-1, in cholesterol-poor domains, and its dedicated sheddases, in cholesterol-rich domains, which could contribute to the inverse relationship between cholesterol abundance and shedding.

The inefficiency of MβCD treatment to remove cholesterol in fibroblastoid HT1080 cells could reflect a particularly low global cholesterol level and/or cholesterol distribution in the plasma membrane *vs.* intracellular organelles in this variant. Cholesterol typically accounts for 20–25% of lipids at the plasma membrane, where it is readily removable by the membrane-impermeant oligosaccharide cyclodextrin cage. Cholesterol is also present in the endocytic recycling compartment and in the Golgi complex, accounting for a residual content insensitive to cyclodextrin treatment (for a review, see ref. 57). Since cholesterol affects both membrane fluidity (57) and stabilization of the submembrane cytoskeleton—and, therefore, membrane deformability (58)—a simple difference in cholesterol plasma membrane level between the two variants could affect both encounter of LRP-1 and its dedicated sheddases and cytoskeleton-dependent cellular functions, such as cell motility.

As an alternative mechanism, a high membrane cholesterol concentration could directly inhibit the shedding activity of MT1-MMP and ADAM-12, as previously reported for MMP inhibition by long-chain unsaturated fatty acids (59). By contrast, a decrease in membrane cholesterol content could stimulate MT1-MMP activity, as described previously for proMMP-2 activation (49), and would thus increase LRP-1 ectodomain shedding. Whatever the mechanism involved, membrane cholesterol appears to control LRP-1-mediated clearance of various ligands, by modulating LRP-1 residence at the cell surface, and thus its endocytic capacity (3). Since the isolated LRP-1 α-chain maintains its activity in Biacore experiments (4), the intact shed LRP-1 ectodomain should compete against the avid clearance mediated by the residual membrane-anchored LRP-1, and further enhance the extracellular level of its multiple ligands as exemplified by MMP-2 and MMP-9 abundance in conditioned medium.

In summary, this study shows that the function of the major endocytic scavenging receptor LRP-1 can be strongly regulated by shedding of its multiligand-binding ectodomain. In HT1080 cells, this process is mediated by two transmembrane metalloproteinases, ADAM-12 and MT1-MMP, and can be tuned by cellular cholesterol levels. Cholesterol could increase compartmentalization between LRP-1 and its dedicated sheddases in distinct domains within the plasma membrane; decrease plasma membrane fluidity, and thereby also limit access of sheddases to their substrate; or directly modulate the activity of membrane-bound sheddases. Regulation of LRP-1 activity by membrane cholesterol sheds new light on the possible role of cholesterol in pathologies in which LRP-1 ligands, including MMPs, are major contributors, such as atherosclerosis. To what extent this concept can be generalized to other cell types and LRP-1 ligands, and is relevant to clinical variations in plasma cholesterol level, deserves further consideration. FJ

The authors thank E. Konradowski and D. Delapière for excellent technical support, as well as Prof. Mark Rider (de Duve Institute, Université Catholique de Louvain, Brussels, Belgium) for editorial assistance. The work was supported by grants from Centre National de la Recherche Scientifique, Contrat de Projets État-Région 2007-2013, and Fonds National pour la Santé ACI 2008 (Cancéropôle Grand-Est Project) (to G.P., S.D. and H.E.); by National Institutes of Health grant AR40994 (to L.T. and H.N.); by the Belgian Fonds de la Recherche Scientifique (FRS/FNRS), the Fondation contre le Cancer and the Direction Générale des Technologies, de la Recherche et de l'Énergie from the Région Wallonne (to A.N.); and by Fonds Spécial de la Recherche of the Université Catholique de Louvain, Fonds de la Recherche Scientifique Médicale, Concerted Research Actions of Communauté Française de Belgique, and Interuniversity Attraction Poles Program (to P.H., P.J.C., and E.M.). C.S. was a recipient of a grant from Belgian FRS/FNRS-Télévie. L.D.A. was a recipient of a grant from the Fonds pour la Formation à la Recherche dans l'Industrie et dans l'Agriculture. P.H. is a research associate at FRS/FNRS.

REFERENCES

1. Lillis, A. P., Van Duyn, L. B., Murphy-Ullrich, J. E., and Strickland, D. K. (2008) LDL receptor-related protein 1: unique tissue-specific functions revealed by selective gene knockout studies. *Physiol. Rev.* **88,** 887–918
2. Emonard, H., Bellon, G., de Diesbach, P., Mettlen, M., Hornebeck, W., and Courtoy, P. J. (2005) Regulation of matrix metalloproteinase (MMP) activity by the low-density lipoprotein receptor-related protein (LRP). A new function for an "old friend". *Biochimie (Paris)* **87,** 369–376
3. Selvais, C., Gaide Chevronnay, H. P., Lemoine, P., Dedieu, S., Henriet, P., Courtoy, P. J., Marbaix, E., and Emonard, H. (2009) Metalloproteinase-dependent shedding of low-density lipoprotein receptor-related protein-1 ectodomain decreases endocytic clearance of endometrial matrix metalloproteinase-2 and -9 at menstruation. *Endocrinology* **150,** 3792–3799
4. Emonard, H., Bellon, G., Troeberg, L., Berton, A., Robinet, A., Henriet, P., Marbaix, E., Kirkegaard, K., Patthy, L., Eeckhout, Y., Nagase, H., Hornebeck, W., and Courtoy, P. J. (2004) Low density lipoprotein receptor-related protein mediates endocytic clearance of pro-MMP-2.TIMP-2 complex through a thrombospondin-independent mechanism. *J. Biol. Chem.* **279,** 54944–54951
5. Herz, J., Clouthier, D. E., and Hammer, R. E. (1992) LDL receptor-related protein internalizes and degrades uPA-PAI-1 complexes and is essential for embryo implantation. *Cell* **71,** 411–421
6. Barnes, H., Ackermann, E. J., and van der Geer, P. (2003) v-Src induces Shc binding to tyrosine 63 in the cytoplasmic domain of the LDL receptor-related protein 1. *Oncogene* **22,** 3589–3597

7. Boucher, P., Liu, P., Gotthard, M., Hiesberger, T., Anderson, R. G. W., and Herz, J. (2002) Platelet-derived growth factor mediates tyrosine phosphorylation of the cytoplasmic domain of the low density lipoprotein receptor-related protein in caveolae. *J. Biol. Chem.* **277,** 15507–15513
8. Degryse, B., Neels, J. G., Czekay, R. P., Aertgeerts, K., Kamikubo, Y. I., and Loskutoff, D. J. (2004) The low density lipoprotein receptor-related protein is a motogenic receptor for plasminogen activator inhibitor-1. *J. Biol. Chem.* **279,** 22595–22604
9. Webb, D. J., Nguyen, D. H. D., and Gonias, S. L. (2000) Extracellular signal regulated kinase functions in the urokinase receptor-dependent pathway by which neutralization of low density lipoprotein receptor-related protein promotes fibrosarcoma cell migration and matrigel invasion. *J. Cell Sci.* **113,** 123–134
10. Dedieu, S., Langlois, B., Devy, J., Sid, B., Henriet, P., Sartelet, H., Bellon, G., Emonard, H., and Martiny, L. (2008) LRP-1 silencing prevents malignant cell invasion despite increased pericellular proteolytic activities. *Mol. Cell. Biol.* **28,** 2980–2995
11. Tamaki, C., Ohtsuki, S., and Terasaki, T. (2007) Insulin facilitates the hepatic clearance of plasma amyloid beta-peptide (1–40) by intracellular translocation of low-density lipoprotein receptor-related protein 1 (LRP-1) to the plasma membrane in hepatocytes. *Mol. Pharmacol.* **72,** 850–855
12. Ceschin, D. G., Sánchez, M. C., and Chiabrando, G. A. (2009) Insulin induces the low density lipoprotein receptor-related protein 1 (LRP1) degradation by the proteasomal system in J774 macrophage-derived cells. *J. Cell. Biochem.* **106,** 372–380
13. Rozanov, D. V., Hahn-Dantona, E., Strickland, D. K., and Strongin, A. Y. (2004) The low density lipoprotein receptor-related protein LRP is regulated by membrane type-1 matrix metalloproteinase (MT1-MMP) proteolysis in malignant cells. *J. Biol. Chem.* **279,** 4260–4268
14. Quinn, K. A., Grimsley, P. G., Dai, Y. P., Tapner, M., Chesterman, C. N., and Owensby, D. A. (1997) Soluble low density lipoprotein receptor-related protein (LRP) circulates in human plasma. *J. Biol. Chem.* **272,** 23946–23951
15. Polavarapu, R., Gongora, M. C., Yi, H., Ranganthan, S., Lawrence, D. A., Strickland, D. K., and Yepes, M. (2007) Tissue-type plasminogen activator-mediated shedding of astrocytic low-density lipoprotein receptor-related protein increases the permeability of the neurovascular unit. *Blood* **109,** 3270–3278
16. Quinn, K. A., Pye, V. J., Dai, Y. P., Chesterman, C. N., and Owensby, D. A. (1999) Characterization of the soluble form of the low density lipoprotein receptor-related protein (LRP). *Exp. Cell Res.* **251,** 433–441
17. Von Arnim, C. A., Kinoshita, A., Peltan, I. D., Tangredi, M. M., Herl, L., Lee, B. M., Spoelgen, R., Hshieh, T. T., Ranganathan, S., Battey, F. D., Liu, C. X., Bacskai, B. J., Sever, S., Irizarry, M. C., Strickland, D. K., and Hyman, B. T. (2005) The low density lipoprotein receptor-related protein (LRP) is a novel beta-secretase (BACE1) substrate. *J. Biol. Chem.* **280,** 17777–17785
18. Liu, Q., Zhang, J., Tran, H., Verbeek, M. M., Reiss, K., Estus, S., and Bu, G. (2009) LRP1 shedding in human brain: roles of ADAM10 and ADAM17. *Mol. Neurodegener.* **4,** 17
19. Tanaka, M., Nanba, D., Mori, S., Shiba, F., Ishiguro, H., Yoshino, K., Matsuura, N., and Higashiyama, S. (2004) ADAM binding protein Eve-1 is required for ectodomain shedding of epidermal growth factor receptor ligands. *J. Biol. Chem.* **279,** 41950–41959
20. Kojro, E., Gimpl, G., Lammich, S., Marz, W., and Fahrenholz, F. (2001) Low cholesterol stimulates the nonamyloidogenic pathway by its effect on the alpha-secretase ADAM 10. *Proc. Natl. Acad. Sci. U. S. A.* **98,** 5815–5820
21. Matthews, V., Schuster, B., Schütze, S., Bussmeyer, I., Ludwig, A., Hundhausen, C., Sadowski, T., Saftig, P., Hartmann, D., Kallen, K. J., and Rose-John, S. (2003) Cellular cholesterol depletion triggers shedding of the human interleukin-6 receptor by ADAM10 and ADAM17 (TACE). *J. Biol. Chem.* **278,** 38829–38839
22. Von Tresckow, B., Kallen, K. J., von Strandmann, E. P., Borchmann, P., Lange, H., Engert, A., and Hansen, H. P. (2004) Depletion of cellular cholesterol and lipid rafts increases shedding of CD30. *J. Immunol.* **172,** 4324–4331
23. Moss, M. L., Bomar, M., Liu, Q., Sage, H., Dempsey, P., Lenhart, P. M., Gillispie, P. A., Stoeck, A., Wildeboer, D., Bartsch, J. W., Palmisano, R., and Zhou, P. (2007) The ADAM10 prodomain is a specific inhibitor of ADAM10 proteolytic activity and inhibits cellular shedding events. *J. Biol. Chem.* **282,** 35712–35721
24. Troeberg, L., Tanaka, M., Wait, R., Shi, Y. E., Brew, K., and Nagase, H. (2002) *E. coli* expression of TIMP-4 and comparative kinetic studies with TIMP-1 and TIMP-2: insights into the interactions of TIMPs and matrix metalloproteinase 2 (gelatinase A). *Biochemistry* **41,** 15025–15035
25. Kashiwagi, M., Tortorella, M., Nagase, H., and Brew, K. (2001) TIMP-3 is a potent inhibitor of aggrecanase 1 (ADAM-TS4) and aggrecanase 2 (ADAM-TS5). *J. Biol. Chem.* **276,** 12501–12504
26. Tyteca, D., D'Auria, L., Van Der Smissen, P., Medts, T., Carpentier, S., Monbaliu, J. C., de Diesbach, P., and Courtoy, P. J. (2010) Three unrelated sphingomyelin analogs spontaneously cluster into plasma membrane micrometric domains. *Biochim. Biophys. Acta* **1798,** 909–927
27. Tanida, S., Joh, T., Itoh, K., Kataoka, H., Sasaki, M., Ohara, H., Nakazawa, T., Nomura, T., Kinugasa, Y., Ohmoto, H., Ishiguro, H., Yoshino, K., Higashiyama, S., and Itoh, M. (2004) The mechanism of cleavage of EGFR ligands induced by inflammatory cytokines in gastric cancer cells. *Gastroenterology* **127,** 559–569
28. Okada, A., Mochizuki, S., Yatabe, T., Kimura, T., Shiomi, T., Fujita, Y., Matsumoto, H., Sehara-Fujisawa, A., Iwamoto, Y., and Okada, Y. (2008) ADAM-12 (meltrin alpha) is involved in chondrocyte proliferation via cleavage of insulin-like growth factor binding protein 5 in osteoarthritic cartilage. *Arthritis Rheum.* **58,** 778–789
29. Robinet, A., Fahem, A., Cauchard, J. H., Huet, E., Vincent, L., Lorimier, S., Antonicelli, F., Soria, C., Crepin, M., Hornebeck, W., and Bellon, G. (2005) Elastin-derived peptides enhance angiogenesis by promoting endothelial cell migration and tubulogenesis through upregulation of MT1-MMP. *J. Cell Sci.* **118,** 343–356
30. Anderegg, U., Eichenberg, T., Parthaune, T., Haiduk, C., Saalbach, A., Milkova, L., Ludwig, A., Grosche, J., Averbeck, M., Gebhardt, C., Voelcker, V., Sleeman, J. P., and Simon, J. C. (2009) ADAM10 is the constitutive functional sheddase of CD44 in human melanoma cells. *J. Invest. Dermatol.* **129,** 1471–1482
31. Foca, C., Moses, E. K., Quinn, M. A., and Rice, G. E. (2000) Differential expression of the alpha(2)-macroglobulin receptor and the receptor associated protein in normal human endometrium and endometrial carcinoma. *Mol. Hum. Reprod.* **6,** 921–927
32. Fröhlich, C., Albrechtsen, R., Dyrskjøt, L., Rudkjaer, L., Ørntoft, T. F., and Wewer, U. M. (2006) Molecular profiling of ADAM12 in human bladder cancer. *Clin. Cancer Res.* **12,** 7359–7368
33. Sounni, N. E., Devy, L., Hajitou, A., Frankenne, F., Munaut, C., Gilles, C., Deroanne, C., Thompson, E. W., Foidart, J. M., and Noël, A. (2002) MT1-MMP expression promotes tumor growth and angiogenesis through an up-regulation of vascular endothelial growth factor expression. *FASEB J.* **16,** 555–564
34. Vassilev, V., Pretto, C. M., Cornet, P. B., Delvaux, D., Eeckhout, Y., Courtoy, P. J., Marbaix, E., and Henriet, P. (2005) Response of matrix metalloproteinases and tissue inhibitors of metalloproteinases messenger ribonucleic acids to ovarian steroids in human endometrial explants mimics their gene- and phase-specific differential control in vivo. *J. Clin. Endocrinol. Metab.* **90,** 5848–5857
35. Cornet, P. B., Galant, C., Eeckhout, Y., Courtoy, P. J., Marbaix, E., and Henriet, P. (2005) Regulation of matrix metalloproteinase-9/gelatinase B expression and activation by ovarian steroids and LEFTY-A/endometrial bleeding-associated factor in the human endometrium. *J. Clin. Endocrinol. Metab.* **90,** 1001–1011
36. Neufeld, E. B., Cooney, A. M., Pitha, J., Dawidowicz, E. A., Dwyer, N. K., Pentchev, P. G., and Blanchette-Mackie, E. J. (1996) Intracellular trafficking of cholesterol monitored with a cyclodextrin. *J. Biol. Chem.* **271,** 21604–21613
37. Bligh, E. G., and Dyer, W. J. (1959) A rapid method of total lipid extraction and purification. *Can. J. Biochem. Physiol.* **37,** 911–917
38. Wu, L., and Gonias, S. L. (2005) The low-density lipoprotein receptor-related protein-1 associates transiently with lipid rafts. *J. Cell. Biochem.* **96,** 1021–1033
39. Kodama, T., Ikeda, E., Okada, A., Ohtsuka, T., Shimoda, M., Shiomi, T., Yoshida, K., Nakada, M., Ohuchi, E., and Okada, Y. (2004) ADAM12 is selectively overexpressed in human glioblastomas and is associated with glioblastoma cell proliferation and shedding of heparin-binding epidermal growth factor. *Am. J. Pathol.* **165,** 1743–1753

40. Edwards, D. R., Handsley, M. M., and Pennington, C. J. (2008) The ADAMs metalloproteinases. *Mol. Aspects Med.* **29,** 258–289
41. Fabre-Lafay, S., Garrido-Urbani, S., Reymond, N., Gonçalves, A., Dubreuil, P., and Lopez, M. (2005) Nectin-4, a new serological breast cancer marker, is a substrate for tumor necrosis factor-alpha-converting enzyme (TACE)/ADAM-17. *J. Biol. Chem.* **280,** 19543–19550
42. Baker, A. H., Edwards, D. R., and Murphy, G. (2002) Metalloproteinase inhibitors: biological actions and therapeutic opportunities. *J. Cell Sci.* **115,** 3719–3727
43. Jacobsen, J., Visse, R., Sorensen, H. P., Enghild, J. J., Brew, K., Wewer, U. M., and Nagase, H. (2008) Catalytic properties of ADAM12 and its domain deletion mutants. *Biochemistry* **47,** 537–547
44. Will, H., Atkinson, S. J., Butler, G. S., Smith, B., and Murphy, G. (1996) The soluble catalytic domain of membrane type 1 matrix metalloproteinase cleaves the propeptide of progelatinase A and initiates autoproteolytic activation. Regulation by TIMP-2 and TIMP-3. *J. Biol. Chem.* **271,** 17119–17123
45. Thevenard, J., Ramont, L., Devy, J., Brassart, B., Dupont-Deshorgue, A., Floquet, N., Schneider, L., Ouchani, F., Terryn, C., Maquart, F. X., Monboisse, J. C., and Brassart-Pasco, S. (2010) The YSNSG cyclopeptide derived from tumstatin inhibits tumor angiogenesis by down-regulating endothelial cell migration. *Int. J. Cancer* **126,** 1055–1066
46. Frisch, S. M. (1994) E1a induces the expression of epithelial characteristics. J. *Cell Biol.* **127,** 1085–1096
47. Ohtani, Y., Irie, T., Uekama, K., Fukunaga, K., and Pitha, J. (1989) Differential effects of α-, β- and γ-cyclodextrins on human erythrocytes. *Eur. J. Biochem.* **186,** 17–22
48. Kilsdonk, E. P. C., Yancey, P. G., Stoudt, G. W., Bangerter, F. W., Johnson, W. J., Phillips, M. C., and Rothblat, G. H. (1995) Cellular cholesterol efflux mediated by cyclodextrins. *J. Biol. Chem.* **270,** 17250–17256
49. Atkinson, S. J., English, J. L., Holway, N., and Murphy, G. (2004) Cellular cholesterol regulates MT1 MMP dependent activation of MMP 2 via MEK-1 in HT1080 fibrosarcoma cells. *FEBS Lett.* **566,** 65–70
50. Huovila, A. P., Turner, A. J., Pelto-Huikko, M., Kärkkäinen, I., and Ortiz, R. M. (2005) Shedding light on ADAM metalloproteinases. *Trends Biochem. Sci.* **30,** 413–422
51. Kveiborg, M., Albrechtsen, R., Couchman, J. R., and Wewer, U. M. (2008) Cellular roles of ADAM12 in health and disease. *Int. J. Biochem. Cell Biol.* **40,** 1685–1702
52. Hikita, A., Yana, I., Wakeyama, H., Nakamura, M., Kadono, Y., Oshima, Y., Nakamura, K., Seiki, M., and Tanaka, S. (2006) Negative regulation of osteoclastogenesis by ectodomain shedding of receptor activator of NF-κB ligand. *J. Biol. Chem.* **281,** 36846–36855
53. Loechel, F., Overgaard, M. T., Oxvig, C., Albrechtsen, R., and Wewer, U. M. (1999) Regulation of human ADAM 12 protease by the prodomain. Evidence for a functional cysteine switch. *J. Biol. Chem.* **274,** 13427–13433
54. Gingras, D., and Béliveau, R. (2010) Emerging concepts in the regulation of membrane-type 1 matrix metalloproteinase activity. *Biochim. Biophys. Acta* **1803,** 142–150
55. Mori, S., Tanaka, M., Nanba, D., Nishiwaki, E., Ishiguro, H., Higashiyama, S., and Matsuura, N. (2003) PACSIN3 binds ADAM12/meltrin alpha and up-regulates ectodomain shedding of heparin-binding epidermal growth factor-like growth factor. *J. Biol. Chem.* **278,** 46029–46034
56. Ehehalt, R., Keller, P., Haass, C., Thiele, C., and Simons, K. (2003) Amyloidogenic processing of the Alzheimer β-amyloid precursor protein depends on lipid rafts. *J. Cell Biol.* **160,** 113–123
57. Ikonen, E. (2008) Cellular cholesterol trafficking and compartmentalization. *Nat. Rev. Mol. Cell. Biol.* **9,** 125–138
58. Byfiels, F. J., Aranda-Espinoza, H., Romanenko, V. G., Rothblat, G. H., and Levitan, I. (2004) Cholesterol depletion increases membrane stiffness of aortic endothelial cells. *Biophys. J.* **87,** 3336–3343
59. Berton, A., Rigot, V., Huet, E., Decarme, M., Eeckhout, Y., Patthy, L., Godeau, G., Hornebeck, W., Bellon, G., and Emonard, H. (2001) Involvement of fibronectin type II repeats in the efficient inhibition of gelatinases A and B by long-chain unsaturated fatty acids. *J. Biol. Chem.* **276,** 20458–20465

Received for publication November 17, 2010.
Accepted for publication April 13, 2011.